NANO LETTERS

2008
Vol. 8, No. 12
4618-4623

High Affinity scFv−Hapten Pair as a Tool for Quantum Dot Labeling and Tracking of Single Proteins in Live Cells

Gopal Iyer,[*,†] Xavier Michalet,[*,†] Yun-Pei Chang,[†] Fabien F. Pinaud,[†,‡] Stephanie E. Matyas,[§] Gregory Payne,[||] and Shimon Weiss[*,†,⊥]

Department of Chemistry & Biochemistry, Department of Hematology/Oncology, David Geffen School of Medicine, Department of Biological Chemistry, David Geffen School of Medicine, and Department of Physiology, David Geffen School of Medicine, UCLA, Los Angeles, California 90024

Received October 24, 2008; Revised Manuscript Received November 11, 2008

ABSTRACT

We describe a general approach to label cell surface proteins using quantum dots (QD) for single-molecule tracking. QDs coated with small-hapten modified peptides are targeted to cell surface fusion proteins containing the corresponding single-chain fragment antibody (scFv). The approach is illustrated with the small hapten fluorescein (FL) and a high-affinity anti-FL scFv fused to two different proteins in yeast and murine neuronal cell line N2a.

Advances in fluorescence microscopy have allowed imaging of single molecules in live cells.[1,2] However, organic dyes and fluorescent proteins (FPs) are prone to rapid photobleaching and fluorescence saturation, limiting the temporal resolution of single-molecule observations. As an alternative fluorophore, quantum dots (QDs) provide brighter and more stable fluorophores that are comparable in size to FPs.[3] However, since QDs are extrinsic probes (not genetically encoded), methods for targeting QDs to proteins of interest are needed. Furthermore, to allow for multicolor imaging, orthogonal targeting approaches must be developed to label different proteins with different color QDs. Antibody−QD conjugates represent one approach for protein labeling.[4] However, the large size of the antibody−QD probe may interfere with protein function or localization. Solutions developed to functionalize proteins with fluorophores could be (and in some cases have been) used with QDs.[1,5,6]

We propose a new labeling strategy that keeps the generality and built-in orthogonality of antibodies but results in much smaller probe sizes. The approach is based on high-affinity single-chain variable fragment antibodies (scFv) against small molecules (or haptens).[7] An scFv and the corresponding hapten constitute affinity partners that can be separately attached to a target protein and QD. We illustrate this approach with the 4M5.3 scFv developed against fluorescein by the Wittrup group.[8] This affinity pair is characterized by a dissociation constant of 48 fM in Low Salt Buffer.[8] We call the resulting QDs *Fl*uorescein-functionalized *pc*-QDs or FL-pc-QDs. Here, we fully characterize this system, demonstrate targeting of single FL-pc-QDs to 4M5.3 scFv displayed on the surface of live yeast and mammalian cells, and show an example of long-term tracking of individual 4M5.3 scFv-PrP fusion proteins in live neuronal cells.

Red-emitting CdSe/CdS/ZnS core−shell QDs were solubilized using various ratios of QD-solubilizing peptides,[9,10] either containing an N-terminal lysine (K-p) and or an N-terminal fluorescein in place of the lysine (FL-p). To prevent nonspecific binding, FL-p coated QDs (FL-pc-QD) containing K-p were functionalized with small molecular weight poly(ethylene glycol) (PEG 330). All samples migrated in agarose gels as narrow bands similar to pure pc-QDs (Figure 1), indicating monodisperse characteristics as previously described.[9,10] The typical diameter of peptide-coated QDs (pc-QDs) was measured by fluorescence correlation spectroscopy (FCS) to be 12 ± 2 nm.[11] The number of FL per QD was estimated by absorption measurements[10] yielding 4, 10, and 25 FL molecules per QD for FL-p:K-p ratios of 10:90, 50:50, and 100:0 (Figure 2 and Supporting Information).

We tested the binding specificity of these FL-pc-QDs against 4M5.3 scFv using a yeast display system.[8] In this

* Corresponding authors: gopal@chem.ucla.edu, michalet@chem.ucla.edu, and sweiss@chem.ucla.edu.
† Department of Chemistry & Biochemistry.
‡ Present address: Dept of Biology, Ecole Normale Supérieure, Paris, France.
§ Department of Hematology/Oncology, David Geffen School of Medicine.
|| Department of Biological Chemistry, David Geffen School of Medicine.
⊥ Department of Physiology, David Geffen School of Medicine.

10.1021/nl8032284 CCC: $40.75
Published on Web 11/20/2008

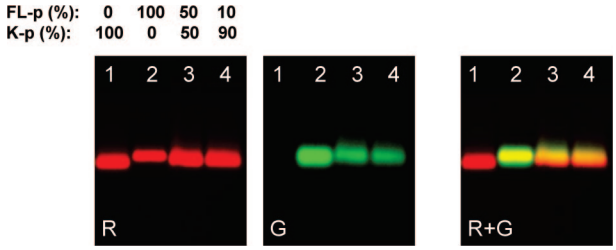

Figure 1. Gel electrophoresis of FL-pc-QDs and pc-QDs samples (red-emitting QDs). The respective percentages of K-p and FL-p used for the preparation of each sample loaded are indicated above each lane. The images show the red (R) and green (G) channel scans as well as an overlay (R + G). All samples migrate at the same speed as pc-QDs (red only) and retain a narrow width, demonstrating monodispersion.

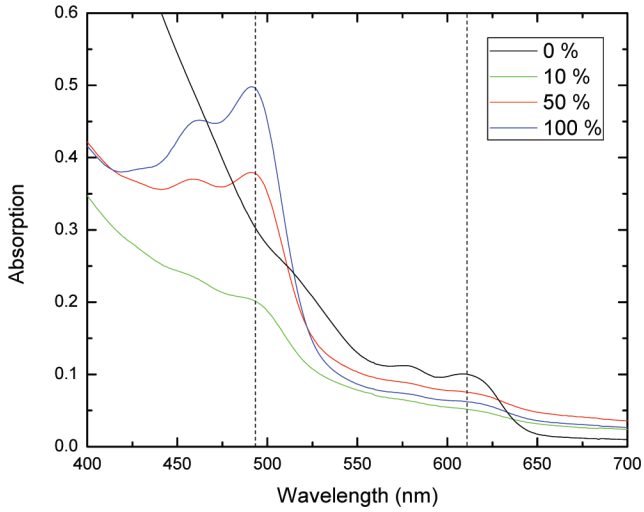

Figure 2. Estimation of the number of FL per FL-pc-QD particle. Absorption spectra for three FL-pc-QD samples (10%, 50%, and 100%) are shown along with a reference "pure" QD sample (0%) used as reference for the application of eq 3 (Supporting Information). The dashed vertical lines indicate the wavelengths used in eq 3 (Supporting Information): 493 and 610 nm.

system, the 4M5.3 scFv sequence is fused to the C-terminus of the Aga2p mating agglutinin and expressed under control of the inducible *GAL1* promoter (Figure 3A). Aga2p is linked by a disulfide bond to Aga1p, which is covalently bound to the cell wall, thus exposing the 4M5.3 scFv at the cell surface (Figure 3B).

In yeast grown in galactose, the induced 4M5.3 scFv was readily detected at the cell surface by immunofluorescence (Figure S1). The ability of yeast displayed 4M5.3 scFv to bind to fluorescein was first established by epifluorescence microscopy using 1 μM FL-conjugated dextran containing several FL molecules per polymer chain (Figure S2A). Binding was dependent on the scFv as no FL-dextran binding was detected in cells grown under noninducing conditions (Figure S2B). Similarly, 10 nM 100% FL-pc-QDs resulted in uniform surface staining of the cells in the green (FL) and red (QD) channels (Figure S2C). Because FL fluorescence is quenched upon binding to 4M5.3 scFv,[8] the green fluorescence cannot be due to binding of free FL or FL-p. To exclude that both signals were due to nonspecific binding of FL-pc-QD to the cell wall, we verified that no green or red signal was detectable for uninduced yeast cells incubated with FL-pc-QD (data not shown). Similar observations were made for the 50% and 10% FL-pc-QD samples. Furthermore, pc-QDs without FL-p molecules did not bind to induced or uninduced yeast cells, demonstrating that binding was mediated by FL (data not shown).

The binding affinity of FL-pc-QD for 4M5.3 scFv was determined using fluorescence-aided cell sorting (FACS) analysis (Figure 4 and Figures S3 and S4 and Supplementary Methods). The average green (FL) and red (QD) signals from gated cells were plotted as a function of concentration. In the absence of induction, no signal above background could be detected in either channel. For induced cells, dissociation constants (K_D) for 10%, 50%, and 100% FL-pc-QD were determined by fitting the FL fluorescence curve to a simple binding model and resulted in $K_D = 3.4 \pm 1.5$ nM ($n = 3$) for 10% FL-pc-QDs, 6.5 ± 3.1 nM ($n = 2$) for 50% FL-pc-QDs and 18.5 ± 3.8 nM ($n = 1$) for 100% FL-pc-QDs. Similar values were obtained from the QD fluorescence signal as well as for FL−dextran binding.

FL-pc-QDs were applied at a concentration (25 pM) much lower than the measured dissociation constant so that single-bound QDs could be resolved for long-term imaging by single-molecule-sensitive stage-scanning confocal microscopy. Because Aga2 is covalently bound to the rigid yeast cell wall, FL-pc-QDs associated with 4M5.3 scFv were static. Figure 3C shows a yeast cell observed in these conditions (see also Movie 1 in Supporting Information) with individual fluorescent spots located at the surface of the cell. To determine whether the observed fluorescent spots corresponded to individual QDs, the excitation laser beam was parked on individual spots and the emitted fluorescence was recorded as a function of time. Figure 3D shows a typical example of time trace recorded in these conditions, with the red fluorescence signal corresponding to the 620 nm emitting QD exhibiting alternating on and off periods characteristic of a blinking QD.[12] The green fluorescence, corresponding to a mixture of FL fluorescence and cell wall autofluorescence, exhibits an exponential decay down to the background level, which is consistent with the presence of a few dozen FL molecules around the QD randomly bleaching as a function of time.

To test our new probe with a mobile target in mammalian cells, 4M5.3 ScFv was fused to the N-terminus of the full length mouse prion protein (PrP) bearing epitope 3F4 and expressed in mouse neuroblastoma cell line N2a (Figure 5A).[13] PrP is anchored to the outer leaflet of cell plasma membrane by a glycosylphosphatidylinositol anchor (Figure 5B). Ensemble confocal imaging of cells labeled with 2 nM FL-pc-QD revealed strong labeling of the cell surface which was absent from untransfected cells, indicating specific labeling of the 4M5.3 ScFv-PrP chimera (Figure S5).

We then imaged the basal membrane of adherent transfected cells labeled with 1−10 pM of FL-pc-QD by total internal reflection fluorescence (TIRF) microscopy. Individual QDs were readily identified as shown in Figure 5C. Individual QD trajectories were reconstructed from movies comprising 1000 frames (100 ms/frame) using published

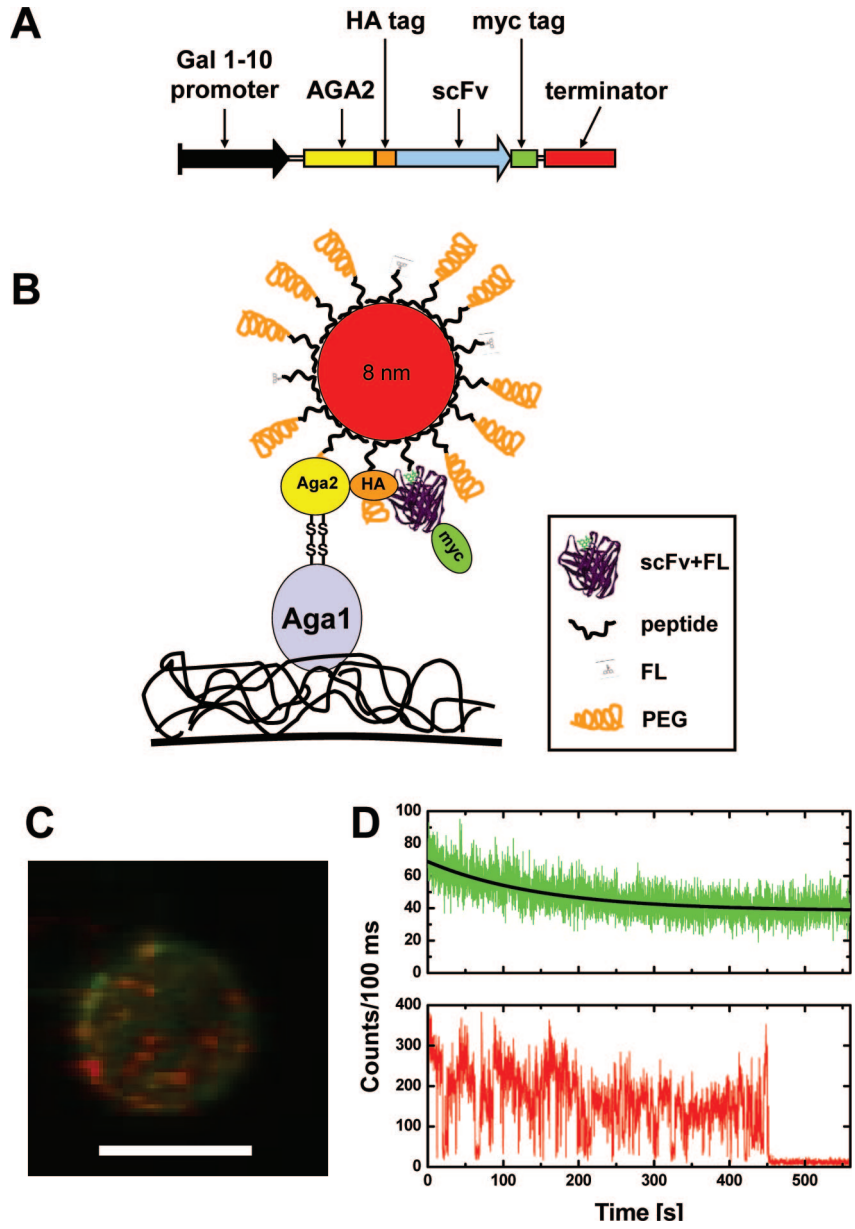

Figure 3. (A) Schematic map of the Aga2-scFv construct (adapted from ref [17]). (B) Cartoon representation of the displayed construct with a bound FL-pc-QD. The QD (red) and 4M5.3 scFv (violet) are represented approximately to scale (structure accession number: 1x9Q). The N-terminus of scFv is bound to the HA tag, while the C-terminus is attached to a myc tag. (C) 3D rendering of a stack of single-molecule confocal sections, showing the punctuated labeling of the yeast surface with individual QDs (Supplementary Movie 1 shows the complete rendering). Scale bar: 5μm. (D) Intensity−time traces corresponding to one of the QDs shown in B. The green signal (FL) decays rapidly (black curve, exponential fit with $\tau = 153$ s) to background autofluorescence level (4 kHz), while the red signal exhibits two-level blinking (25 kHz) for >7 min. Excitation: 3 μW at 488 nm, pinhole: 50 μm.

single-particle tracking algorithm.[14] We identified several diffusion regimes in transfected cells (free, confined, directed, slow, and fast), which will be described in detail in a forthcoming publication. Figure 5D presents an example of a trajectory exhibiting two distinct diffusion regimes. The emission intensity of QDs (Figure 5E) followed during their diffusion exhibited the typical on/off blinking behavior of QDs, as reported previously, confirming that single FL-pc-QDs bound to a scFv-PrP were observed.

Taken together, our results demonstrate that QD-based scFv labeling in cells displays specificity, high affinity, versatility, and compatibility with single-molecule imaging.

Although the multivalency of our FL-pc-QD probes raises the possibility that a single QD could associate with several surface scFvs, consideration of the geometries of binding suggests that each QD binds only one scFv molecule in both yeast and N2a cells. In the case of yeast, each cell displays $\sim 5 \times 10^4$ scFv molecules.[8] Assuming a random distribution on the yeast surface (5 μm diameter), the scFv density is thus $\sim$1 per 1500 nm^2 $\sim$ 40 $\times$ 40 nm^2. Since each FL-pc-QD is $\sim$12 nm in diameter, the probability of two scFvs being close enough to bind to a single QD is therefore negligible. The situation is different in N2a cells, where scFv-PrP can freely diffuse along the membrane. A simple

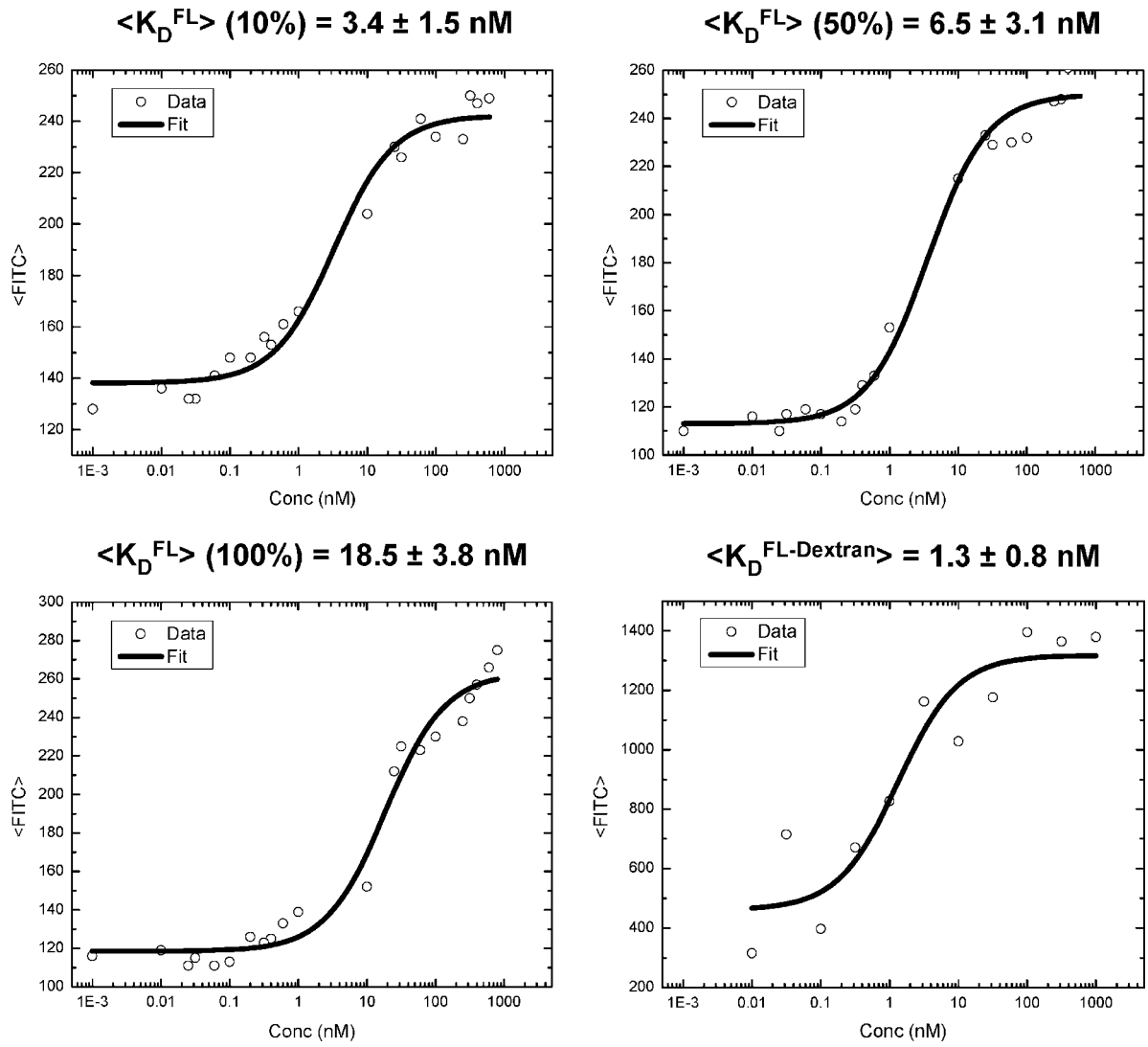

Figure 4. Representative FACS measurement of the dissociation constant K_D between 4M5.3 scFv displayed on yeast cells and FL-pc-QDs with different FL-p:K-p coverage (10:90, 50:50, 100:0 and control: FL-dextran). For each condition, a representative curve of the average FITC fluorescence signal per cell at a given concentration of FL-pc-QD is shown. The average fitted value of the dissociation constant for this condition is indicated above each curve.

geometrical calculation presented in Supporting Information indicates that even in these conditions, it is very unlikely that more than one scFv molecule binds to a given FL-pc-QD. In particular, the probability that this happens is essentially zero for FL-pc-QD coated with 10% FL−peptides.

It should be straightforward to apply our strategy with other scFv−hapten pairs chosen among the existing pairs developed for biotechnological purposes, such as for instance digoxin and analogues.[7] It would be advantageous to extend it to affinity pairs involving variable fragments (Fv) or a variable fragment of heavy chain (V_H), further reducing the footprint of the peptide domain added to the targeted protein.[7] Finally, although we used peptide coating to functionalize QDs, this approach could be used with any other QD-functionalization protocol permitting the addition of small haptens to QDs. Having multiple orthogonal affinity pairs will offer the possibility to label and track different proteins using different color QDs. The main advantage of this affinity pair based labeling approach is the simplicity of target labeling, which only requires adding the probe to the cell growth medium prior to observation. In particular, unlike chemical or enzymatic approaches, it does not require the addition of precisely adjusted mixtures of diverse components at usually large concentrations, and does not involve any rinsing steps. One potential drawback of our approach is that it requires genetic engineering of DNA vectors. However, this is something that has become routine practice in most laboratories since the development of fluorescent protein tagging of proteins.[15] Moreover, unlike FP-tagged proteins, the level of *labeled* proteins can be controlled independently of the protein expression level, by externally adjusting the concentration of QD probes or the duration of incubation. Finally, our approach is particularly suited for surface proteins labeling; labeling of cytoplasmic proteins or proteins expressed in internal cell compartments may be limited by the stability of the scFv structure in reducing environments and could therefore require the specific engineering of more stable scFv molecules.[16] Targeting internal proteins in any

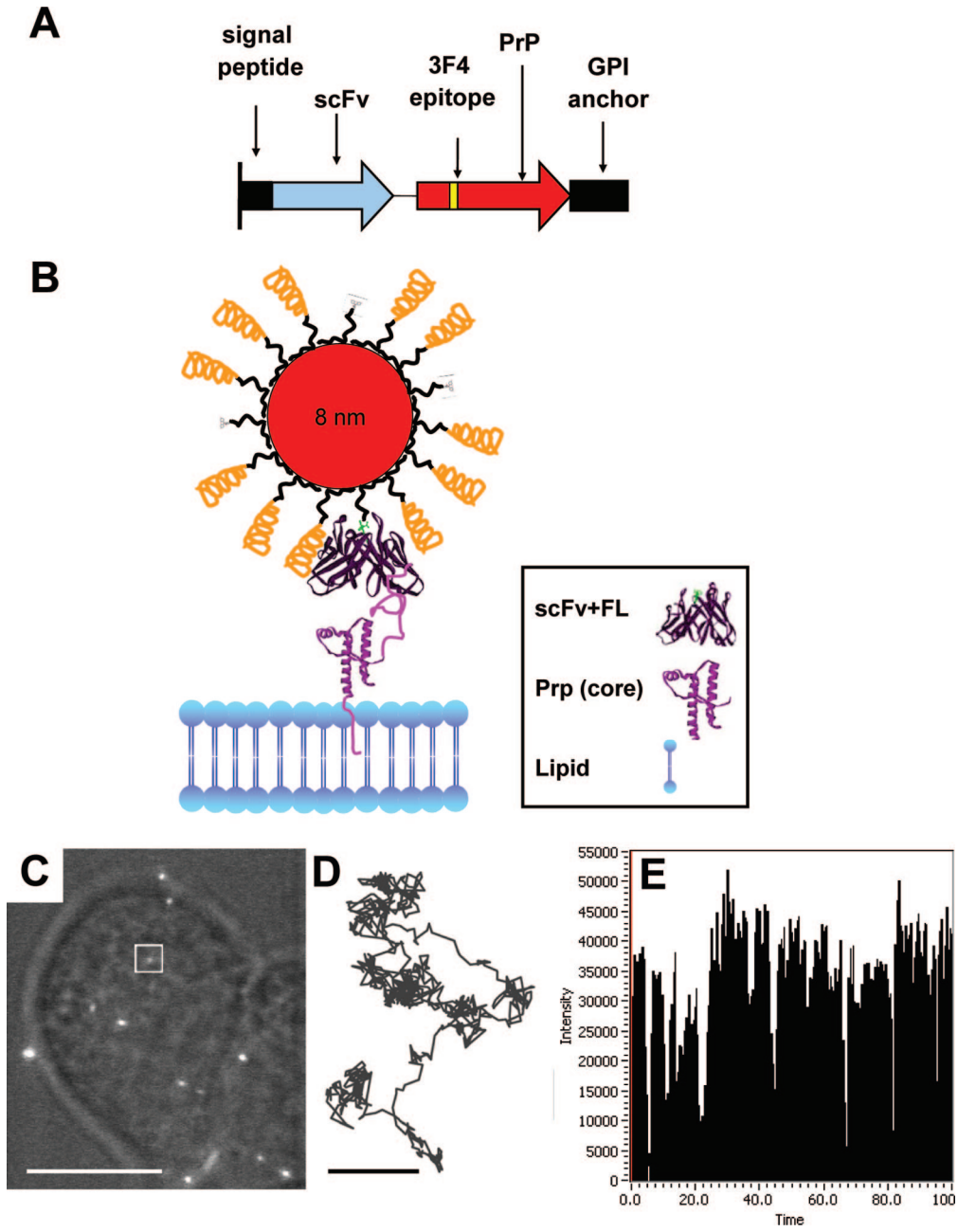

Figure 5. (A) Schematic map of the scFv-PrP construct. 4M5.3 is fused to the N-terminus of the full-length mouse PrP sequence by a short linker sequence. (B) Cartoon representation of a scFv-PrP anchored in the membrane's outer leaflet of an N2a cell via its GPI-anchor, with a bound FL-pc-QD. The QD and 4M5.3 scFv, PrP, and GPI-anchor are represented approximately to scale. The 4M5.3 scFv (violet) is oriented 90° from its orientation in Figure 3B. (C−E) Single-particle tracking of scFv-PrP in live neuroblastoma cells. Live N2a cells stably expressing the GPI-anchored scFv-PrP grown on polylysine-coated glass coverslips were stained with 1 pM FL-pc-QDs for 10 min and rinsed with buffer. (C) DIC image with overlaid red fluorescence signal (white dots). (D) 1000 frames single-QD trajectory of the QD indicated by the white square in (B). (E) Intensity time trace (camera counts/frame) along the trajectory exhibiting a blinking pattern typical of a single QD. Scale bar: (C) 10 μm, (D) 1 μm.

case will require overcoming the still challenging obstacle of QD internalization and targeting.

In summary, we have demonstrated a labeling method using small hapten-functionalized QDs that should be widely applicable, is well suited for single-protein tracking experiments, and offers the same generality and ease of use as FP-labeling of proteins with the added advantages of allowing long-term and multiplexed visualization of individual proteins.

Acknowledgment. We thank Professor Wittrup for providing the 4M5.3 scFv plasmid, Professor Lindquist for the mouse PrP plasmid, and Dr. Thomas Dertinger for help with FACS data import. We acknowledge the help of Dr. Ingrid Schmid, supervisor of the UCLA Jonsson Comprehensive Cancer Center (JCCC) and Center for AIDS Research Flow Cytometry Core Facility that is supported by National Institutes of Health awards CA-16042 and AI-28697, and by the JCCC, the UCLA AIDS Institute, and the David

Geffen School of Medicine at UCLA. Ensemble confocal imaging was performed at the UCLA/CNSI Advanced Light Microscopy Shared Facility. This work was supported by NIH/NIBIB BRP Grant 5-R01-EB000312 and the NSF, The Center for Biophotonics, an NSF Science and Technology Center managed by the University of California, Davis, under Cooperative Agreement PHY0120999.

Supporting Information Available: Details of experimental methods, a more detailed discussion of the results, additional supporting figures, and a video. This material is available free of charge via the Internet at http://pubs.acs.org.

References

(1) Giepmans, B. N. G.; Adams, S. R.; Ellisman, M. H.; Tsien, R. Y. *Science* **2006**, *312* (5771), 217–224.
(2) Joo, C.; Balci, H.; Ishitsuka, Y.; Buranachai, C.; Ha, T. *Annu. Rev. Biochem.* **2008**, *77*, 51–76.
(3) Michalet, X.; Pinaud, F. F.; Bentolila, L. A.; Tsay, J. M.; Doose, S.; Li, J. J.; Sundaresan, G.; Wu, A. M.; Gambhir, S. S.; Weiss, S. *Science* **2005**, *307*, 538–544.
(4) Dahan, M.; Levi, S.; Luccardini, C.; Rostaing, P.; Riveau, B.; Triller, A. *Science* **2003**, *302* (5644), 442–445.
(5) Chen, I.; Ting, A. Y. *Curr. Opin. Biotechnol.* **2005**, *16* (1), 35–40.
(6) Foley, T. L.; Burkart, M. D. *Curr. Opin. Chem. Biol.* **2007**, *11* (1), 12–19.
(7) Sheedy, C.; MacKenzie, R. C.; Hall, J. C. *Biotechnol. Adv.* **2007**, *25* (4), 333–352.
(8) Boder, E. T.; Midelfort, K. S.; Wittrup, K. D. *Proc. Natl. Acad. Sci. U.S.A.* **2000**, *97*, 10701–10705.
(9) Pinaud, F.; King, D.; Moore, H.-P.; Weiss, S. *J. Am. Chem. Soc.* **2004**, *126*, 6115–6123.
(10) Iyer, G.; Pinaud, F.; Tsay, J.; Weiss, S. *Small* **2007**, *3* (5), 793–798.
(11) Doose, S.; Tsay, J. M.; Pinaud, F.; Weiss, S. *Anal. Chem.* **2005**, *77* (7), 2235–2242.
(12) Nirmal, M.; Dabbousi, B. O.; Bawendi, M. G.; Macklin, J. J.; Trautman, J. K.; Harris, T. D.; Brus, L. E. *Nature* **1996**, *383*, 802–804.
(13) Ma, J.; Lindquist, S. *Proc. Natl. Acad. Sci. U.S.A.* **2001**, *98* (26), 14955–14960.
(14) Michalet, X.; Lacoste, T. D.; Weiss, S. *Methods* **2001**, *25* (1), 87–102.
(15) Tsien, R. Y. *Annu. Rev. Biochem.* **1998**, *67*, 509–544.
(16) Wörn, A.; Plückthun, A. *J. Mol. Biol.* **2001**, *305* (5), 989–1010.
(17) Feldhaus, M. J.; Siegel, R. W.; Opresko, L. K.; Coleman, J. R.; Weaver Feldhaus, J. M.; Yeung, Y. A.; Cochran, J. R.; Heinzelman, P.; Colby, D.; Swers, J.; Graff, C.; Wiley, H. S.; Wittrup, K. D. *Nat. Biotechnol.* **2003**, *21*, 163–170.

NL8032284